Zeitschrift: Schweizerische mineralogische und petrographische Mitteilungen = Bulletin suisse de minéralogie et pétrographie

Band: 82 (2002)

Heft: 2: Diagenesis and Low-Grade Metamorphism

Artikel: Chloritoid composition and formation in the eastern Central Alps : a comparison between Penninic and Helvetic occurrences

Autor: Rahn, Meinert K. / Steinmann, Marc / Frey, Martin

DOI: https://doi.org/10.5169/seals-62373

SCHWEIZ. MINERAL. PETROGR. MITT. 82, 409–426, 2002

Chloritoid composition and formation in the eastern Central Alps: a comparison between Penninic and Helvetic occurrences

by *Meinert K. Rahn*[1, *], *Marc Steinmann*[2] and *Martin Frey*[3] *(deceased)*

Abstract

Chloritoid occurs in Middle Cretaceous shales (Bündnerschiefer) of the Tomül nappe in the Safien valley. Compositional and textural data of chloritoid are compared with nearby occurrences at Curaglia/Mutschnengia (sedimentary cover of the Gotthard nappe) and at Kunkels Pass (Helvetic Autochthonous). At the Tomül nappe profile, the observed mineral assemblage is phengitic mica-chlorite-quartz-chloritoid-paragonite-mixed layer phengite/paragonite. Textures indicate syn- to post-kinematic growth of chloritoid with respect to the main schistosity. Temperatures derived from chloritoid-chlorite and chlorite thermometry suggest metamorphic peak conditions of 400 ± 50 °C pre-D2, i.e. before Early Oligocene, but these have to be considered with caution due to high Mn contents in chloritoid.

Comparison with neighbouring occurrences indicates very similar, but more Mn-depleted chloritoid compositions at Kunkels Pass and Curaglia. In these localities, chloritoid forms rosettes growing across the main schistosity, which indicates post-kinematic growth after the Early Oligocene. Whereas temperatures obtained for Curaglia are similar to those for the occurrence in the Tomül nappe, they are distinctly lower (300–350 °C) for Kunkels Pass, where chlorite does not coexist with chloritoid.

The formation of chloritoid is discussed for various bulk rock compositions on the basis of a four-component multisystem. The Al contents, the amount of carbonate, and a value of $X_{Mg} < 0.45$ turn out to be important factors. The formation of chloritoid in Bündnerschiefer is assumed to be due to a reaction muscovite + chlorite → chloritoid + celadonite; alternatively, its formation at the expense of high-pressure ferrocarpholite may be suggested. However, unlike the observations in other parts of the North Penninic Bündnerschiefer, no observations in favour of the formation of chloritoid at high pressures, due to ferrocarpholite breakdown, have been made in the Tomül profile studied.

Keywords: Chloritoid, chlorite thermometry, North Penninic, Infrapenninic, Helvetic.

1. Introduction

Chloritoid (cld) appears as an important index mineral in Al-rich shales at the onset of the greenschist facies (BUCHER and FREY, 1994). In the Central Alps, the reaction pyrophyllite (prl) + chlorite (chl) → chloritoid (cld) + quartz (qtz) + H_2O was mapped as a cld-in isograd by FREY and WIELAND (1975). In the area they investigated, located in the eastern Central Alps, this reaction isograd roughly follows the southern end of the Helvetic belt (Fig. 1), suggesting that cld should be common in Al-rich Penninic Bündnerschiefer further south, because of their slightly higher metamorphic grade compared to the Helvetic units further north (FREY and FERREIRO MÄHLMANN, 1999). However, only few reports of cld have been published from this area so far (NIGGLI and NIGGLI, 1965; OBERHÄNSLI et al., 1995).

The presence of typical high-pressure (HP) minerals such as ferrocarpholite, glaucophane and lawsonite within the sediments of the North Penninic palaeogeographic belt (OBERHÄNSLI et al., 1995; GOFFÉ and BOUSQUET, 1997; BOUSQUET et al., 1998) raises interesting questions about the metamorphic history of the Helvetic and adjacent North Penninic units, and about the continuity of the metamorphic pattern across the Penninic

[1] Institut für Mineralogie, Petrologie und Geochemie, Albert-Ludwigs-Universität, Albertstrasse 23b, D-79104 Freiburg, Germany.
* Present address: HSK, CH-5232 Villigen-HSK, Switzerland. <rahn@hsk.psi.ch>
[2] Département de Géosciences, UFR Sciences et Techniques, Université de Franche-Comté, 16 route de Gray, F-25030 Besançon cedex, France. <marc.steinmann@univ-fcomte.fr>
[3] Mineralogisch-Petrographisches Institut, Universität Basel, Bernoullistrasse 30, CH-4056 Basel, Switzerland.

thrust front, as suggested by the latest compilation of metamorphic data (FREY et al., 1999). While HP indicators have been reported from North Penninic units within the Engadine window (BOUSQUET et al., 1998), and from the Peiden slice (OBERHÄNSLI et al., 1995) north of the Adula nappe (Fig. 1), such evidence is absent in the Helvetic belt. This fact is attributed to a Late Cretaceous/Early Tertiary subduction event affecting the sediments and subordinate magmatic rocks of the former Valais trough subsequent to their incorporation into the Alpine orogeny, while sedimentation was ongoing in the Helvetic realm (PFIFFNER, 1986).

While FREY (1969), FREY and WIELAND (1975) and MAYERAT (1986) have discussed the presence of cld within Helvetic and Infrapenninic units as part of a post-kinematic metamorphic overprint, cld within North Penninic units was proposed to result from the breakdown of ferrocarpholite at pressures above 0.7 GPa (GOFFÉ and BOUSQUET, 1997; BOUSQUET et al., 1998). The purpose of this paper is a detailed comparison of compositional and textural aspects of chloritoid occurring in different tectonic units of the eastern Central Alps. The question of how cld is formed is discussed on the basis of bulk rock and mineral compositions on one side, and textural aspects on the other.

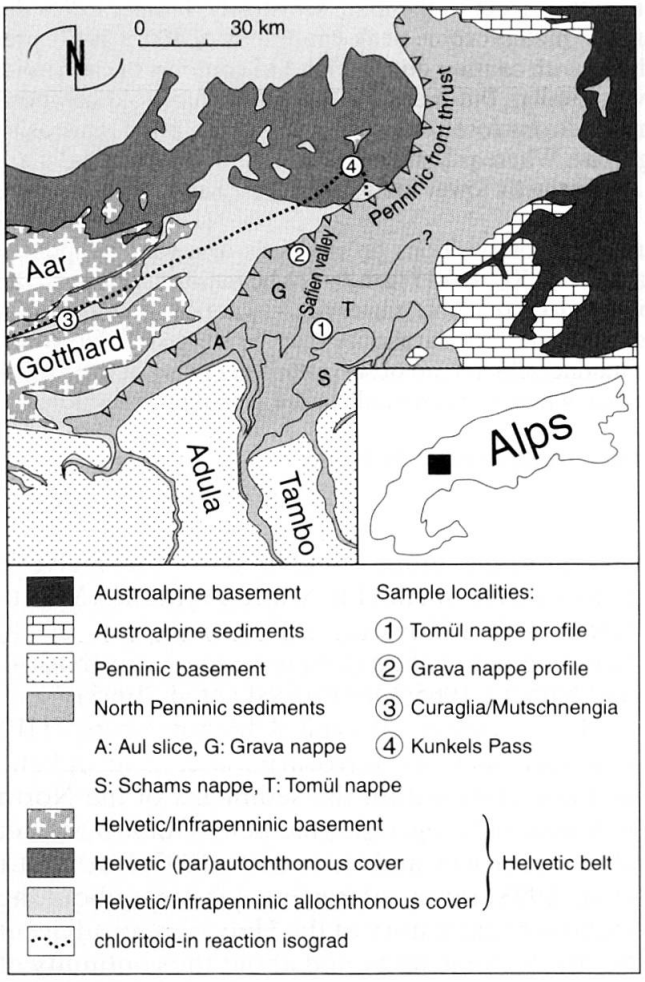

Fig. 1 Tectonic map of the eastern Central Alps, modified after TRÜMPY (1980) and STEINMANN (1994a,b). The three sample localities belong to three different palaeotectonic units, the Helvetic (Kunkels Pass), the Infrapenninic (Curaglia/Mutschnengia), and the North Penninic (Tomül nappe) sedimentation realm. The age variation among the sampled sediments ranges from upper Triassic to mid Cretaceous.

2. Geologic Setting and Sample Localities

The Central Alps are characterised by a relatively strict southwards and upwards succession of tectonic units, which represents the result of a Tertiary continent-continent collision subsequent to Early Mesozoic rifting and Late Cretaceous to Tertiary convergence. During rifting two oceanic realms were formed, and later closed by convergence. The two colliding continental plates, the Eurasian plate in the N (the present-day Helvetic belt), and the Apulian microplate in the S with the present-day Austroalpine/Southalpine units represent the lowermost and uppermost units, respectively, of the actual Alpine edifice. The Penninic units in-between are remnants of an extended southern ocean (Piemont-Liguria), an intermediate "terrane" (STAMPFLI and MARCHANT, 1997) or crystalline rise (Briançonnais), and a northern ocean (Valais trough) of debated size and extension (STAMPFLI and MARCHANT, 1997; OBERHÄNSLI, 1994, STEINMANN and STILLE, 1999). In the actual Alpine edifice, these form the South, Middle, and North Penninic units, respectively. According to their palaeogeographic origin and time of incorporation into the Alpine orogeny, each of these main units have undergone distinct structural and metamorphic histories, which in part can be inferred from the metamorphic pattern at the present surface (FREY et al., 1999).

The South Penninic units underwent shortening and metamorphism since the beginning of the closure of the Tethys ocean some 100 Ma ago (STAMPFLI et al., 1998). It is assumed that a large portion of the South Penninic oceanic substratum was subducted during convergence. Remnants of this oceanic crust are represented by ophiolites (Zermatt-Saas Fee, Aosta ophiolites, Platta nappe, Arosa zone, Ramosch slice, see BEARTH, 1967; TRÜMPY, 1988), and serpentinites (Malenco, TROMMSDORFF et al., 1993). The Middle Penninic units are present as basement nappes (Adula, Tambo, Fig. 1) with some residual Mesozoic sediments, and as sediment nappes, which have been

detached from their crystalline substratum along Triassic evaporites. Accretion of the Middle Penninic units probably took place during the Early Tertiary as suggested by the presence of Eocene flysch in the overthrusted North Penninic units (ZIEGLER, 1956).

Some of the North Penninic units are characterised by widespread basaltic intercalations and local occurrences of pillow lava and gabbro. However, complete sequences of oceanic crust, comparable to those in South Penninic units, are lacking. Most of the North Penninic basalts can be interpreted as submarine lava flows (STEINMANN, 1994a, b). Nd–Sr isotope and trace element data clearly indicate a depleted mantle origin for these basalts suggesting that, despite the absence of a typical ophiolite sequence, the North Penninic basin was underlain by oceanic crust (STEINMANN and STILLE, 1999). Dominant in the North Penninic units are "Bündnerschiefer" (STEINMANN, 1994 a, b), pelitic to calciclastic metasediments of low metamorphic grade. They consist of a sediment pile, up to 2.5 km thick, and form the Grava nappe and overlying Tomül nappe of the study area (Fig. 1). In the Bündnerschiefer of eastern Switzerland, maximum metamorphic conditions vary from high diagenesis-subgreenschist facies in the NE to amphibolite facies in the S (FREY et al., 1999). There is growing evidence, however, that at least parts of the eastern Valais trough sediments underwent a high-pressure (HP) overprint (OBERHÄNSLI et al., 1995; BOUSQUET, 1998; BOUSQUET et al., 1998) reaching eclogite facies conditions in the S near San Bernardino Pass (Neu Wahli, e.g. RING, 1992; OBERHÄNSLI, 1994).

The Helvetic units comprise a polymetamorphic basement and a monometamorphic sedimentary sequence (Permian to Oligocene). These were incorporated in the Alpine orogeny by burial and nappe stacking after the Middle Oligocene. The Helvetic units were buried below Penninic and Austroalpine units and underwent a metamorphic overprint reaching lowermost greenschist facies in the south (FREY and FERREIRO MÄHLMANN, 1999). Various metamorphic discontinuities along the nappe boundaries reveal that part of the thrusting was post-metamorphic (e.g. RAHN et al., 1995). In the eastern Central Alps, Helvetic and Penninic units are separated from each other by the Penninic front thrust (Fig. 1) that approximately follows the valley of the Anterior Rhine. Metamorphic conditions on each side of the valley suggest a common history for the Late Tertiary metamorphic overprint (FREY and FERREIRO MÄHLMANN 1999). The HP event in the North Penninic units is thought to have taken place contemporaneously to eclogite formation in the Adula nappe (BECKER, 1992; GEBAUER et al., 1992; OBERHÄNSLI et al., 1995). Hints to a HP overprint are missing in the Helvetic belt.

The transition from the Helvetic to the Penninic palaeogeographic realm, thus from continental margin platform to open sea sedimentation in the Mesozoic, is transient. Flysch units incorporated in the Helvetic belt (Sardona, Blattengrat flysch) are commonly attributed to Ultrahelvetic or "Infra-" to "Sub"-Penninic environments, and are thought to be associated with crystalline basement units such as the Gotthard nappe (LEHNER et al., 1997). The Gotthard nappe itself might

Table 1 List of sample localities from the four investigated areas. Localities are indicated by rectangular Swiss map coordinates (1 unit = 1 km, Swiss capital Berne = 600/200).

Section name	Sample abbreviation	Formation name	Base of section	altitude	Top of section	altitude
Tomül nappe Bündnerschiefer						
Carnusabach	CA	Bärenhorn Fm.	744.610/171.020	1470 m	745.120/170.880	1630 m
Gross Rüti	GR	Uppermost Bärenhorn Fm.	744.950/170.720	1585 m	744.850/170.600	1620 m
Mittelbärg	MB, Cld 1–10	Nollaton Fm.	743.180/169.540	1820 m	743.750/168.950	2200 m
Chräjenchöpf	CC1–CC15	Nollakalk Fm.	746.400/169.025	2180 m	746.550/169.500	2460 m
Chräjenchöpf	CC16–CC 24	Carnusa Fm.	746.550/169.500	2460 m	746.580/168.900	2640 m
Grava nappe Bündnerschiefer						
Turisch-Tobel	TT	Bärenhorn-Carnusa Fm.	742.175/181.850	1050 m	742.800/179.230	1830 m
Gotthard nappe cover						
Curaglia	MR P 288	Quartenschiefer	708.670/170.360	1290 m	–	–
Mutschnengia	MR P 304–308	Quartenschiefer Stgir formation	707.680/169.920	1410 m	707.480/170.160	1560 m
Helvetic autochthonous cover						
Kunkels Pass	MF 1207	Bommerstein series	751.025/195.025	1100 m	–	–

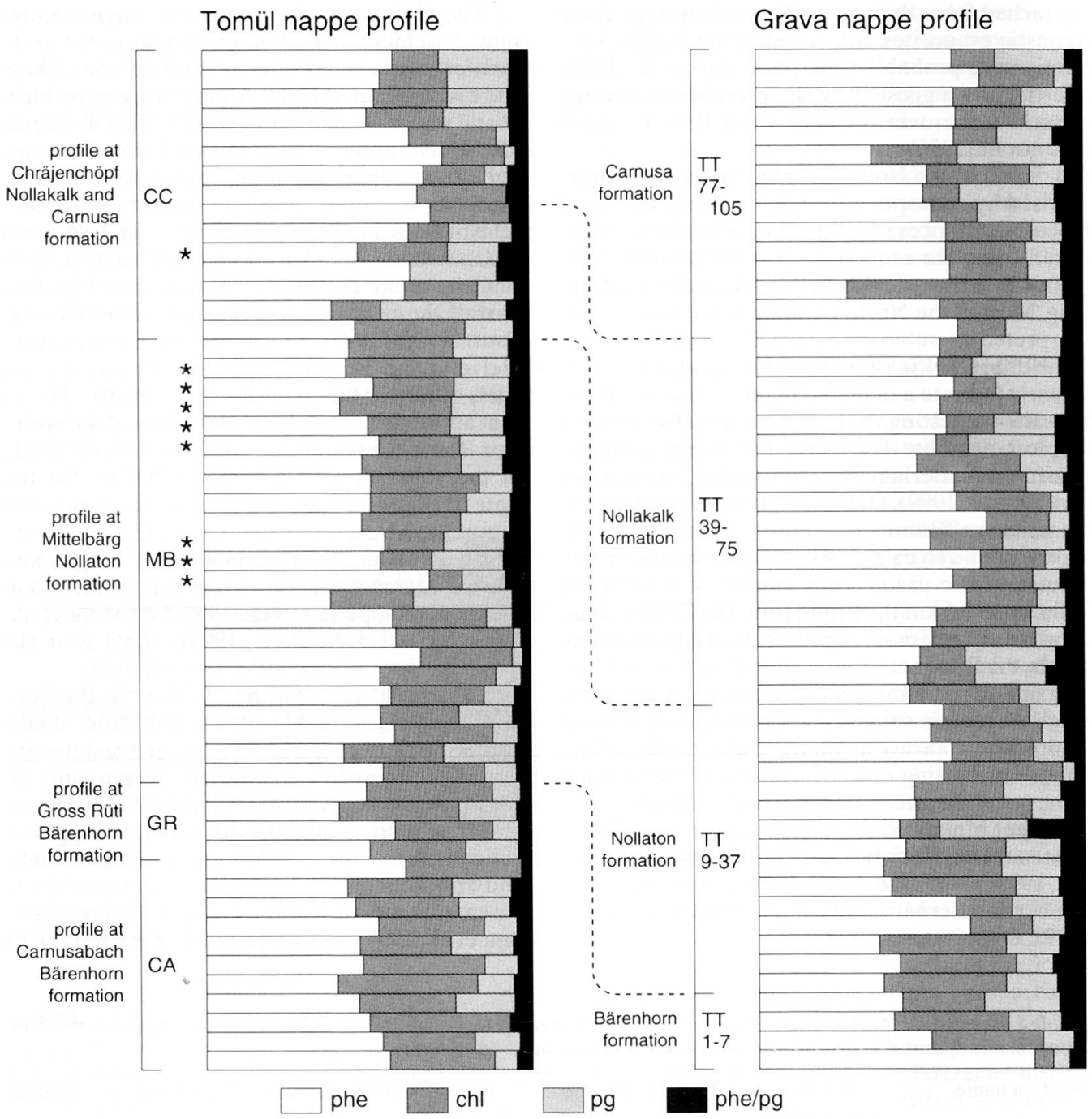

Fig. 2 Relative amount of sheet silicate content from the decarbonised clay fraction of the Tomül nappe and Grava nappe profiles. Samples containing chloritoid are marked with asterisks (only found in Tomül nappe). Quantification of the phases is based on XRD peak heights, and has a relative accuracy of ±2–3%. A more detailed description of the profiles is given in STEINMANN (1994a,b)

have been linked directly to typical crystalline units from the Lepontine dome such as the Simano and Adula nappe (PROBST, 1980; ETTER, 1987), which are surrounded by North Penninic Bündnerschiefer. During Tertiary shortening, these units became a narrow succession of crystalline basement nappes with only restricted zones of metasediments in-between, while further to the east, the Alpine edifice is today dominated by sedimentary units (Fig. 1).

The North Penninic units were sampled along two complete stratigraphic sections across the Grava nappe and the overlying Tomül nappe in the course of a detailed stratigraphic analysis of Bündnerschiefer (STEINMANN, 1994a, b). The stratigraphic polarity in both sections is normal. The section "Turisch-Tobel" across the Grava nappe is located in the Anterior Rhine valley, east of Ilanz, directly above the Penninic front thrust. A section across the Tomül nappe has been com-

piled from four sub-sections taken between Safien valley and Piz Beverin, SW of Glas Pass (Tomül nappe profile). Detailed sampling localities are listed in Table 1, and an overview on the sampled stratigraphic units of the two Bündnerschiefer sections is given in Fig. 2. The strategy in the field was to sample the most fine-grained shale interval every 30 ± 10 m. All 53 Grava samples were cld-free, whereas cld was discovered in 7 of the 53 Tomül samples. All cld-bearing samples originate from the shaly Middle Cretaceous Nollaton formation (Fig. 2), which was re-sampled (samples Cld 1-10) for this study.

We report on chemical and mineralogical bulk rock analyses from the Bündnerschiefer succession of the Tomül nappe profile and on microprobe data of three cld-bearing samples of the Tomül Nollaton samples (Cld. 7-9). For comparison, a combination of similar lithologies with and without cld were sampled nearby: (a) at Turisch-Tobel, a Bündnerschiefer profile in the Grava nappe (STEINMANN, 1994a, b), (b) one sample in the classic cld locality at Curaglia (TRÜMPY, 1980), combined with 13 samples at the little road to Mutschnengia and Stagias, including Upper Triassic Quartenschiefer and Lower Liassic black shales with and without cld, all from the Gotthard nappe sedimentary cover, and (c) one sample from the Kunkels Pass (MF 1207, Middle Jurassic Bommerstein formation, autochthonous cover of the Helvetic crystalline basement, FREY and WIELAND, 1975) (Fig. 1). Samples were investigated by optical means, XRD and XRF, and selected specimens from cld-bearing lithologies were used for analysis by electron microprobe.

3. Methods

For XRD, XRF and ICP analyses, subsamples were crushed by disk mill. For XRD investigation, rock powders were sedimented on glass slides. Analyses at the University of Basel were performed on a PHILIPS PW-1360 with a Cu tube at 40 kV and 25 mA, including a Ni filter, no monochromator, and slits of 1°, 0.2 mm, and 1°. Data were accumulated at a scan speed of 2° 2θ min^{-1} with a step increment of 0.05° 2θ. At the University of Freiburg, XRD analyses were performed on a Bruker AXS D8 Advance at 40 kV and 30 mA. Data accumulation was at a step size of 0.017° and a step time of 1 s. Relative contents of the silicate minerals were estimated using measured peak heights above background. To test the influence of sample thickness, sample TT41 from the Grava Bündnerschiefer was measured six times with increasing amounts of sedimented material. For a slide thickness of 1–6 mg cm^{-2} no trend was observed, and the mean composition was 45.7 ± 1.2 vol% phe, 20.5 ± 1.5 % chl, 21.7 ± 1.5 % pg, and 12.0 ± 0.8 vol% mixed-layer pg/phe. The indicated (1σ) standard deviations are assumed to represent typical errors in our mineral contents data due to slide thickness variation.

XRF analysis of major elements was performed for glass pellets, melted at 1100 °C for 8 minutes using 1g of rock powder and 4g of a $Li_2B_4O_7/LiBO_2$ mixture. Analysis were performed on a Philips 2404 at the Institute of Mineralogy, Petrology and Geochemistry at Freiburg University (sample numbers "Cld", MRP 288, 304a–308, MF 1207) and on a PW 1404 at the EMPA Dübendorf (Tomül samples CA, GR, MB, and CC). For ICP analyses 300 mg of sample powder were dried at 110 °C, ignited at 1000 °C, fused with Li_2BO_4, and then dissolved in a HNO_3-glycerine solution for analysis in a ARL 3500 ICP atomic emission spectrometer at the CNRS-CGS laboratory in Strasbourg (Grava samples TT). $CaCO_3$ and total organic carbon (TOC) contents of Tomül and Grava Bündnerschiefer were determined coulometrically at the ETH in Zürich (Coulomat Ströhlein Labortechnik).

Mineral analyses were performed in a Cameca SX-100 electron microprobe at 15 kV acceleration voltage and 20 nA beam current. The elements Si, Ti, Al, Cr, Fe, Mn, Mg, Ca, Ba, Na and K were standardised against natural and synthetic standards. The contents of Cr and Ba never exceeded 0.05 wt% and are neglected. Fe was calculated as FeO.

4. Results

4.1. FIELD AND TEXTURAL RELATIONSHIPS

A total of 116 Tomül and Grava Bündnerschiefer samples and 14 samples from the Infrapenninic Gotthard sedimentary cover at Curaglia/Mutschnengia were analysed by bulk rock XRD analysis. Mineral assemblages in Tomül samples comprise major quartz, phengite (phe), and chlorite (chl), minor albite (ab), paragonite (pg) and paragonite/phengite (pg/phe) mixed layer sensu FREY (1969), variable carbonate contents (calcite and occasionally dolomite), accessory graphitic organic matter (PETROVA et al., 2002) and hematite or pyrite. The occurrence of chloritoid (cld) is restricted to samples of low carbonate content. The presence of pg/phe was determined using XRD (FREY, 1969) and microprobe analysis of Na- and K-rich white mica flakes. Pyrophyllite (prl) and biotite are completely absent in the investigated samples. After carbonate removal and separation

of the <2 μm fraction, the estimated phengite content varies from 39 to 74 vol%, chlorite has a variation from 10 to 43%, paragonite from 0 to 38%, and the estimated pg/phe mixed layer fraction ranges between 0 and 9% (Fig. 2) for the Bündnerschiefer samples of the Tomül nappe. Slight compositional trends, with samples getting richer in muscovite but poorer in chlorite, up-section are observed. The Grava samples show no cld, but otherwise identical assemblages and similar ranges in mineral contents.

At the Tomül nappe profile, cld is present only in samples of the shaly Nollaton formation and one sample of the Nollakalk formation. Cld-bearing samples are not characterised by especially low or high contents of other minerals (except for carbonate). Note that in Bündnerschiefer, cld was not visible in any of the cld-bearing specimens. The frequent field occurrence in both Bündnerschiefer profiles of knotted schists (called "Leopardenschiefer" in the literature), with dark patches of up to 2 mm in diameter, do not indicate the presence of cld. Microscope and microprobe investigations revealed that these black knots are carbonate-rich aggregates surrounded by dark organic matter.

For 14 samples from the Infrapenninic sediments at Curaglia/Mutschnengia, a common mineral paragenesis of phe-chl-qtz±pg±pg/phe±carb ±cld±ab was observed. Quartenschiefer (Triassic) tend to be dominated by sheet silicates, while Liassic shales are often ab- or qtz-dominated, thus originated from more psammitic sediments. The occurrence of cld is restricted to carbonate-free samples from the Quartenschiefer , close to a porous layer of Triassic dolomites and Liassic quartzites, while no cld has been found in the Liassic shales. In the Infrapenninic samples, cld is occasionally visible in hand specimen as sub-mm size black dots in a commonly dark matrix. Cld is absent in purple or green Quartenschiefer, and cld-bearing samples show very small amounts of ab. For the Kunkels Pass samples, FREY and WIELAND (1975) reported a paragenesis of phe-phe/pg-cld-qtz ± organic matter, and the investigated sample has estimated volume contents of 40% white mica, 35% qtz, 10–15% cld, with minor carbonate, albite, and apatite. That study reported a limitation of cld occurrence to shaly, carbonate-poor layers which is similar to cld occurrences in the Bündnerschiefer.

4.2. MINERAL COMPOSITION AND MICROTEXTURES

Electron microprobe analyses were performed in three samples from the North Penninic Tomül nappe profile (Cld 7-9), one sample from the Helvetic autochthonous sediments north of the Kunkels Pass (MF 1207) and one sample from the Quartenschiefer of Curaglia (MR P 288). Measured minerals include cld, chl, ms, and pg; representative cld and chl analyses of each sample are given in Table 2. In the following, each mineral is characterised by its composition at each locality.

Microtextures of *chloritoid* within the North Penninic cld schists (Tomül nappe) are markedly different from those of Curaglia and Kunkels Pass: cld within the Bündnerschiefer shales forms long flakes parallel to the main schistosity (D1, Fig. 4a). In qtz-rich layers cld also forms long prisms growing at high angles to the main schistosity (Fig. 4a, right). Cld in Quartenschiefer at Curaglia and in Jurassic shales at Kunkels Pass forms bundles of prisms, rosettes and flower structures, up to 300 μm in diameter, growing across the main schistosity (Fig. 4b to d). Prism cores are commonly rich of qtz inclusions (Fig. 4d), themselves aligned parallel to the external main schistosity; rims are mainly inclusion-free. Cores and rims of the cld prisms show no difference in chemical composition.

All cld from the Tomül nappe profile are Fe-rich, and X_{Mg} (=Mg/(Mg+Fe)) values vary between 0.08 and 0.12 (n = 26). At Curaglia, X_{Mg} in cld varies between 0.10 and 0.14 (n = 18), at Kunkels Pass between 0.06 and 0.12 (n = 10). The Kunkels Pass and Curaglia chloritoids are very low in MnO (<0.25 wt%), while some chloritoids from the Bündnerschiefer show similar occupation of the octahedral site by Mn and Mg (Fig. 3a). Whereas the Bündnerschiefer cld analyses show no correlation between Fe and Mg contents, samples from Curaglia and Kunkels Pass show a distinct Fe–Mg exchange. In addition, Mn contents in cld increase with the amounts of Mn in the bulk rock (Fig. 3b).

Chlorite is a major constituent of the rock matrix in cld-bearing samples from the Tomül nappe and Curaglia, but it is completely absent in samples from Kunkels Pass (FREY and WIELAND, 1975). Chlorite shows a restricted variation in X_{Mg}: 0.40–0.49 for the Tomül samples, 0.42–0.47 at Curaglia. The amount of tetrahedral Al varies between 2.5 and 2.9 p.f.u (calculated for 28 oxygens, Table 2). Chlorite forms small flakes oriented parallel to the main schistosity. At the Tomül profile, chl occurs as random flakes together with cld in qtz-rich layers of <1 mm thickness. Non-aligned chlorites are equal in composition to the aligned ones, indeed none of the different populations show any chemical zoning. Chlorite crosscutting the schistosity, such as reported from the Bündnerschiefer (e.g. WEH, 1998), has not been observed in any of the investigated localities.

In all locations studied *white micas* are the main constituents of the matrix apart from qtz and chl. Contrasts in BSE images occasionally allow the detection of phengitic and paragonitic sheets. In the Quartenschiefer at Curaglia phengitic flakes were too small for analysis without contamination by other phases, in particular qtz (Fig. 4c and d). It is assumed that intergrowths between phengite and paragonite are likely to be present in all samples, with scales from the size of single 10Å sheet intergrowth (as indicated by the presence of mixed-layer pg/phe X-ray reflections) to a sheet thickness of several tens of μm (as indicated by the presence of large pg flakes in the samples from the Tomül profile). While phe/pg mixed layer reflections can be found at all three

Table 2 Representative chlorite and chloritoid analyses from the Tomül nappe profile, Curaglia and Kunkels Pass, and corresponding temperature calculations for the chloritoid-chlorite thermometer (VIDAL et al., 1999) and chl thermometer (CATHELINEAU, 1988).

	Tomül nappe Bündnerschiefer						Curaglia		Kunkels Pass	
Sample	Cld 07	Cld 07	Cld 08	Cld 08	Cld09	Cld 09	MR P 288	MR P 288	MF 1207	MF 1207
analysis	cld5	cld6	cld3	cld7	cld7	cld10	cld12	cld20	cld1	cld4
SiO_2	24.01	23.66	23.78	24.94	24.29	24.49	24.41	25.37	23.52	23.95
TiO_2	0.11	0.03	0.07	0.00	0.21	0.02	0.03	0.02	0.02	0.03
Al_2O_3	39.67	39.69	39.81	42.29	41.68	41.48	41.98	41.90	39.83	40.24
FeO	22.92	22.55	23.67	23.37	22.87	23.05	24.88	24.55	25.21	25.10
MnO	2.43	2.20	1.65	1.67	1.54	1.47	0.18	0.13	0.15	0.11
MgO	1.42	1.55	1.54	1.60	1.38	1.64	1.71	1.73	1.37	1.58
CaO	0.00	0.00	0.00	0.01	0.03	0.03	0.04	0.02	0.01	0.00
Na_2O	0.01	0.01	0.01	0.01	0.01	0.00	0.02	0.01	0.00	0.00
K_2O	0.02	0.04	0.04	0.05	0.04	0.04	0.02	0.01	0.01	0.01
Σ	90.60	89.74	90.57	93.95	92.06	92.22	93.26	93.74	90.12	91.01
calculated on the basis of 12 oxygens										
Si	2.034	2.019	2.015	2.021	2.008	2.021	1.997	2.056	2.004	2.016
Ti	0.007	0.002	0.004	0.000	0.013	0.001	0.002	0.01	0.001	0.002
Al	3.960	3.992	3.976	4.040	4.061	4.036	4.049	4.001	4.000	3.992
Fe^{2+}	1.623	1.609	1.678	1.584	1.581	1.592	1.702	1.664	1.797	1.767
Mn	0.174	0.159	0.118	0.115	0.108	0.103	0.013	0.009	0.011	0.008
Mg	0.179	0.197	0.195	0.193	0.170	0.202	0.208	0.208	0.174	0.198
Ca	0.000	0.000	0.000	0.001	0.003	0.003	0.003	0.002	0.001	0.000
Na	0.002	0.002	0.002	0.002	0.001	0.000	0.002	0.001	0.000	0.000
K	0.002	0.004	0.004	0.005	0.005	0.004	0.002	0.001	0.001	0.001
	chl5	chl6	chl3	chl7	chl7	chl10	chl12	chl20		
SiO_2	24.15	24.75	24.43	24.69	24.31	25.12	25.81	24.49		
TiO_2	0.04	0.12	0.06	0.01	0.03	0.05	0.07	0.07		
Al_2O_3	22.26	23.56	23.16	24.81	24.84	23.95	25.38	25.32	no	no
FeO	26.60	25.70	25.49	26.31	26.67	26.06	25.56	25.76	chlorite	chlorite
MnO	0.75	0.72	0.46	0.50	0.45	0.43	0.06	0.04		
MgO	11.61	10.83	12.57	11.68	11.16	11.76	12.40	12.16		
CaO	0.01	0.00	0.00	0.01	0.01	0.02	0.00	0.00		
Na_2O	0.01	0.03	0.00	0.02	0.00	0.02	0.03	0.01		
K_2O	0.04	0.15	0.02	0.06	0.06	0.03	0.02	0.04		
Σ	85.47	85.87	86.20	88.09	87.53	87.44	89.33	87.89		
calculated on the basis of 28 oxygens										
Si	5.284	5.342	5.245	5.192	5.158	5.312	5.293	5.133		
Ti	0.007	0.019	0.010	0.002	0.004	0.008	0.010	0.011		
Al	5.740	5.993	5.861	6.147	6.213	5.970	6.134	6.255		
Fe^{2+}	4.867	4.639	4.577	4.626	4.733	4.609	4.384	4.516		
Mn	0.139	0.132	0.084	0.089	0.080	0.078	0.010	0.007		
Mg	3.787	3.485	4.023	3.663	3.532	3.707	3.789	3.799		
Ca	0.002	0.000	0.000	0.003	0.003	0.004	0.000	0.000		
Na	0.004	0.013	0.000	0.009	0.000	0.007	0.011	0.000		
K	0.011	0.041	0.005	0.016	0.016	0.008	0.006	0.004		
$T_{cld\text{-}chl}$	404 °C	437 °C	387 °C	423 °C	407 °C	430 °C	402 °C	414 °C		
T_{chl}	375 °C	366 °C	382 °C	390 °C	396 °C	371 °C	374 °C	400 °C		

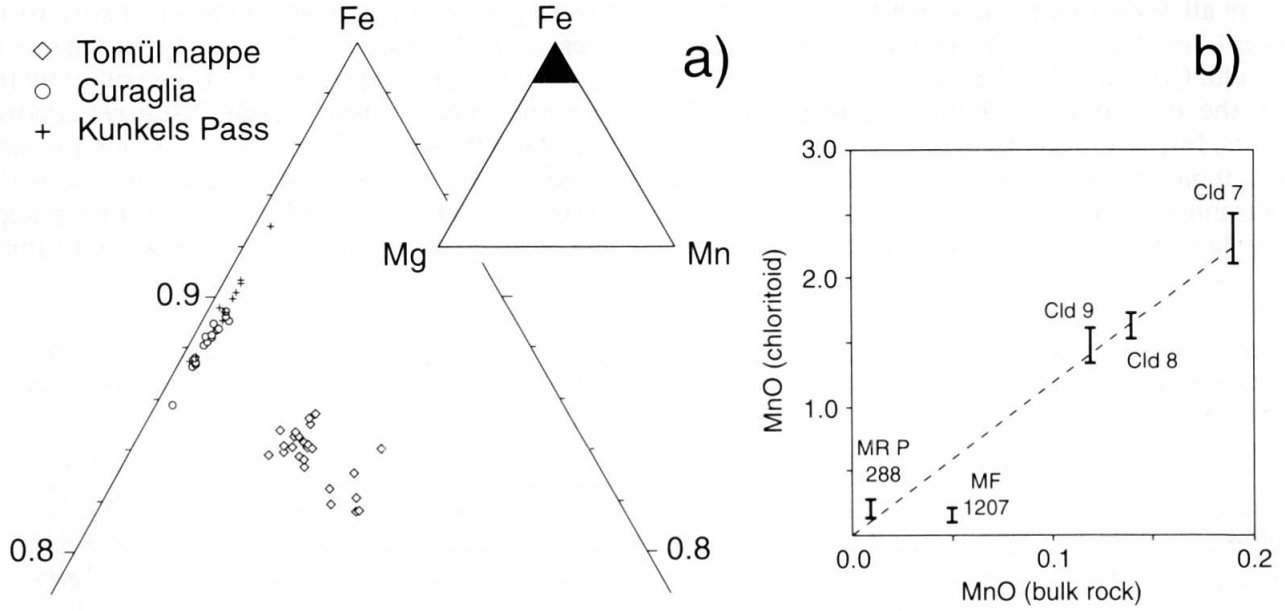

Fig. 3 Diagrams illustrating the Mn content in chloritoid: (a) Fe-Mg-Mn ternary plot with chloritoid analyses from the Tomül nappe, Curaglia, and Kunkels Pass samples. While chloritoids from Curaglia and Kunkels Pass are very low in Mn, chloritoids from the Tomül nappe profile have Mn contents in the range of the Mg. (b) Dependence of the chloritoid Mn content on bulk rock Mn.

localities, pg reflections are absent at Kunkels Pass (FREY and WIELAND, 1975). Flakes of phengitic sheets are ubiquitous in the matrix and are aligned parallel to the main schistosity. Despite their homogeneous texture, phengitic white micas reveal distinct compositional variations, ranging from Si = 3.00–3.43 (based on 11 oxygens) for Tomül samples, and Si = 3.05–3.27 for Kunkels Pass phengite. The increase in Si, however, correlates with a decrease in Na and total interlayer cations, and an increase in (Fe+Mn+Mg) content (Fig. 5). In the Tomül samples one pg-rich analyses shows a $X_{Pa} = 0.67$.

Quartz is ubiquitous with a grain size of <5–50 μm. Grains elongated in the main schistosity indicate for all samples that quartz grains underwent elongation due to pressure solution processes during deformation at high temperature. Cld-bearing samples have little to no carbonate. Strongly weathered pyrite cubes are a common accessory in Quartenschiefer, while hematite is present in small amounts in the Bündnerschiefer. Other accessory phases include apatite, frequently needle-shaped with atoll structure, tourmaline, and an unspecified polymorph of TiO_2. Pyrophyllite, kaolinite, talc, biotite, and ferrocarpholite have not been found in any of the samples.

4.3. BULK ROCK COMPOSITION

Major element compositions were determined for 63 samples from the Tomül profile, 53 samples from the Grava profile, 14 samples from Curaglia/Mutschnengia, and one from Kunkels Pass. Samples were divided into cld-bearing and non cld-bearing groups. Samples from the Tomül nappe profile exhibit a large variation in chemical composition, mainly due to variations in quartz and carbonate contents. All cld-bearing Tomül samples originate from the shaly Nollaton formation (with one exception, Fig. 2) and are characterised by low $CaCO_3$ (< 0.66%) and elevated TOC (> 0.3%) contents. However, not all samples with comparable $CaCO_3$ and TOC contents contain cld. When projected through white mica (for this projection, an endmember composition of muscovite was assumed due to the lack of a reasonable phengite analysis in cld-bearing samples, Fig. 5, and no analysis in cld-free samples) and plotted in an AFM diagram (Fig. 6a), bulk chemical compositions vary between an Al-rich Fe-dominated end member at one side (located within a three-phase field determined by cld, an Al-rich phase and chl), and an Al-poor Mg-dominated end member, below the compositional range for chlorites on the other. Cld-bearing samples are only found above the tie-line bundle between measured cld and chl compositions, and below a maximum X_{Mg} of 0.45. One exception to this rule is the Helvetic sample MF 1207 from Kunkels Pass (no chl!), which plots just below the corresponding cld analyses. Note that all samples of the cld-free Grava Bündnerschiefer plot to the right of the 0.45 X_{Mg}-line in spite of $CaCO_3$ and TOC contents comparable to those of cld-bearing Tomül samples.

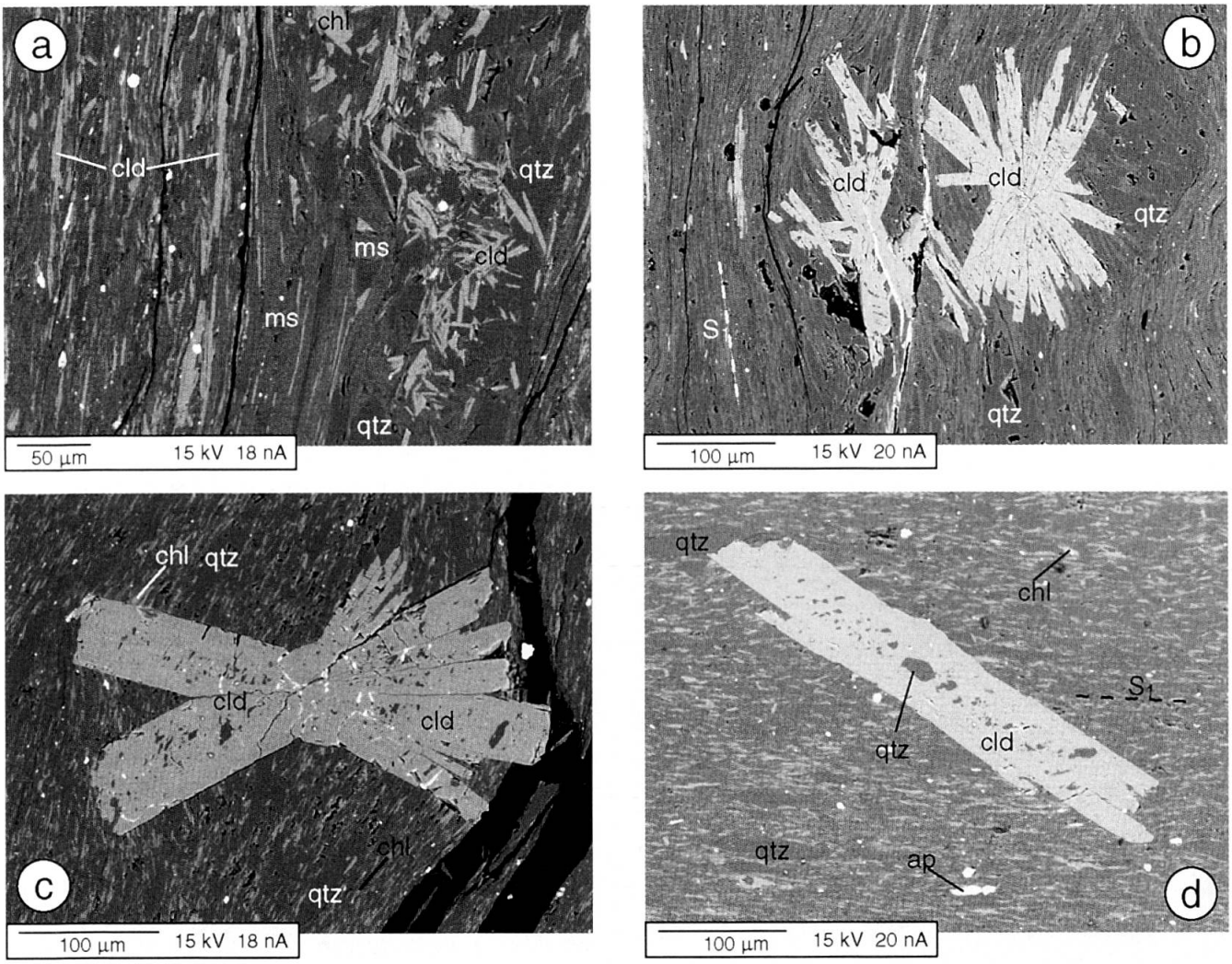

Fig. 4 Back-scattered electron images of microtextures within chloritoid-bearing samples from Tomül nappe, Curaglia and Kunkels Pass. (a) Aligned and non-aligned chloritoid from the Tomül nappe profile. The matrix is dominated by phengitic muscovite (sample Cld 09). (b) Chloritoid (cld) rosettae within fine-grained quartz (qtz)-phengite matrix from Kunkels Pass (sample MF 1207). (c) Chloritoid bundle in quartz-chlorite (chl)-phengite matrix from Curaglia (sample MR P 288). (d) Single chloritoid prism with an inclusion-rich core, but nearly inclusion-free rim from Curaglia (sample MR P 288).

A similar pattern is found for a series of 14 samples from the Infrapenninic Gotthard nappe cover at Curaglia-Mutschnengia (Fig. 6b). While the more marly samples plot below the cld-chl tie-lines, the cld-bearing samples (only Quartenschiefer) all fall into the three-phase field (cld-chl-A).

5. Discussion

5.1. THE TIME OF CLD FORMATION

Textures from the three different localities suggest that cld formed either syn-main schistosity (D1, Bündnerschiefer) or post-main schistosity (Gotthard nappe cover, Helvetic autochthonous cover). This raises the questions, whether the main schistosities represent the same structural event at all localities, and whether aligned and non-aligned chloritoid in the Tomül nappe profile may be the result of two distinct structural or metamorphic events. The structural relationships in the Tomül nappe Bündnerschiefer are identical with those described by SCHMID et al. (1990) and SCHREURS (1991, 1993) in the overlying Schams nappes (STEINMANN 1994a, b). According to these authors, the main schistosity in the Bündnerschiefer was formed during the D1 or Ferrera phase. D1 includes all structural features developed pre-D2, which is the Niemet-Beverin structural event (D2 of SCHMID et al., 1990). In Bündnerschiefer further east, WEH (1998) and WEH and FROITZHEIM (2001) distinguished two structural phases D1a and D1b. D2 typically appears as crenulation cleavage in thin sections and is thought to be of Early Oligocene age (SCHMID et al. 1997).

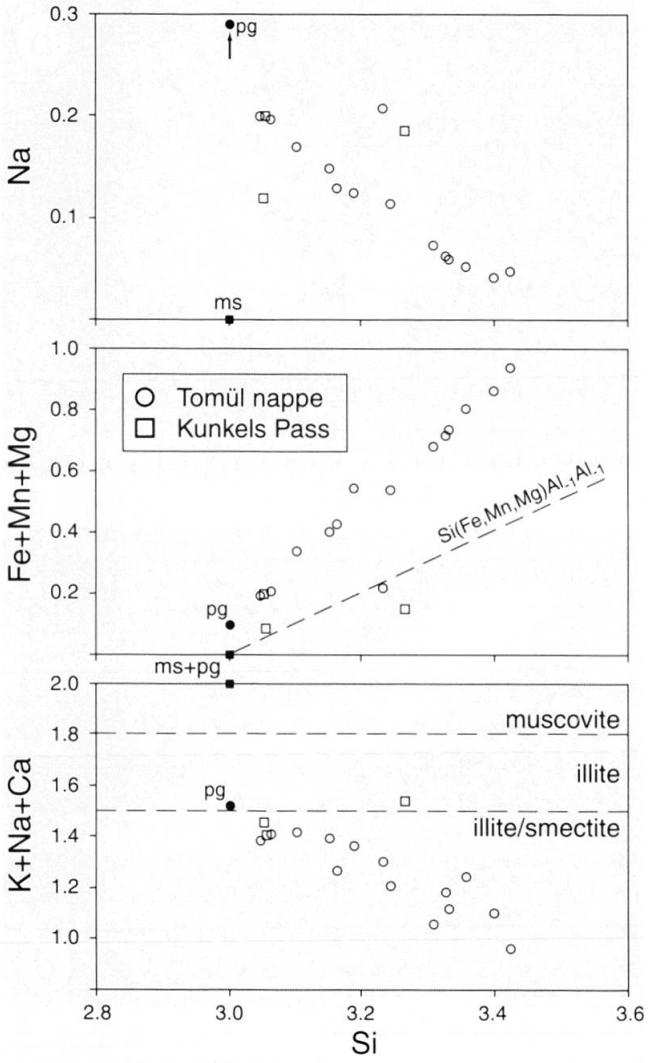

Fig. 5 Chemical variation of white micas from Tomül nappe Bündnerschiefer and Kunkels Pass Jurassic shales. The observed variation in Si content does not result from a celadonite exchange, but an exchange with one Si being exchanged simultaneously with two (Fe+Mn+Mg).

The observed non-aligned cld and chl in qtz-rich layers raise the question whether this texture may be related to a crenulation cleavage post-D1, e.g. as a result of D2. However, no crenulation of the D1 planes is observed in any of the cld-bearing samples in hand specimen. Textures show that the non-aligned cld and chl never grow across qtz-layers, i.e. across minerals aligned in the D1 schistosity (Fig. 4a). Thus, this lack of alignment in the qtz-rich layers may be explained by strain partitioning rather than by growth of a second generation of cld. Because D1 may be a mulitphase event, the time of cld growth here is bracketed by the age of the Ferrrara phase in general (Eocene, SCHMID et al., 1997) and the time of the Niemet-Beverin phase (D2, Early Oligocene). Because D1 in Bündnerschiefer may not be a single structural event (WEH, 1998; WEH and FROITZHEIM, 2001), and includes anything pre-D2, cld formation is not further specified in relation to a previous high-pressure overprint sensu OBERHÄNSLI et al. (1995) and BOUSQUET et al. (1998). The question of whether aligned (syn-D1) and non-aligned (possibly post-D1) chloritoid and chlorite represent distinct populations, derived from two separate metamorphic events, cannot be answered with certainty. For the Tomül nappe profile, however, the two populations are part of the same assemblage and are indistinguishable in composition and metamorphic grade of formation. This supports the idea that cld formed in a single event before Early Oligocene.

In Curaglia and Kunkels Pass samples, cld grew across the main schistosity. The corresponding deformation phase, the Calanda phase (MILNES and PFIFFNER, 1977) has been dated further to the north in the Glarus Alps (HUNZIKER et al., 1986) to be of Early Oligocene age. In the Kunkels pass area, structures of the Calanda phase predominate, whereas structures of the earlier Pizol and Cavistrau phases are commonly absent in the lower parautochthonous units (PFIFFNER, 1986). For the Gotthard nappe cover, the main schistosity was created during overthrust of the Gotthard nappe on top of the external Tavetsch massif (MAYERAT, 1986; PFIFFNER, 1986). According to thin section observations, cld forms pre- to syn-D2, a crenulation cleavage visible within schistose lithologies of the sedimentary cover (MAYERAT, 1986). Consequently, cld growth in the Helvetic and Infrapenninic sediments was syn- to post-Early Oligocene, and the time of its its formation cannot be related to cld in Bündnerschiefer.

5.2. THERMOMETRY

The assemblage cld-chl from the Tomül nappe profile and at Curaglia can be used for the estimation of metamorphic temperatures which, according to VIDAL et al. (1999), are nearly independent of pressure. 22 cld-chl pairs from samples Cld 07 (n = 6), Cld 08 (n = 7), and Cld 09 (n = 9) of the Tomül profile yield an average temperature of 415 ± 50 °C (2σ), while for Curaglia a set of 4 chl-cld pairs give temperatures of 410 ± 30 °C (Table 2).

A detailed analysis of the relevant distribution coefficient reveals that chloritoid from all samples is generally restricted in X_{Mg} variation, while chlorite from Bündnerschiefer of the Tomül nappe shows more scatter in X_{Mg} (Fig. 7). This may be due to retrograde recrystallisation or late weathering of the samples. No difference, howev-

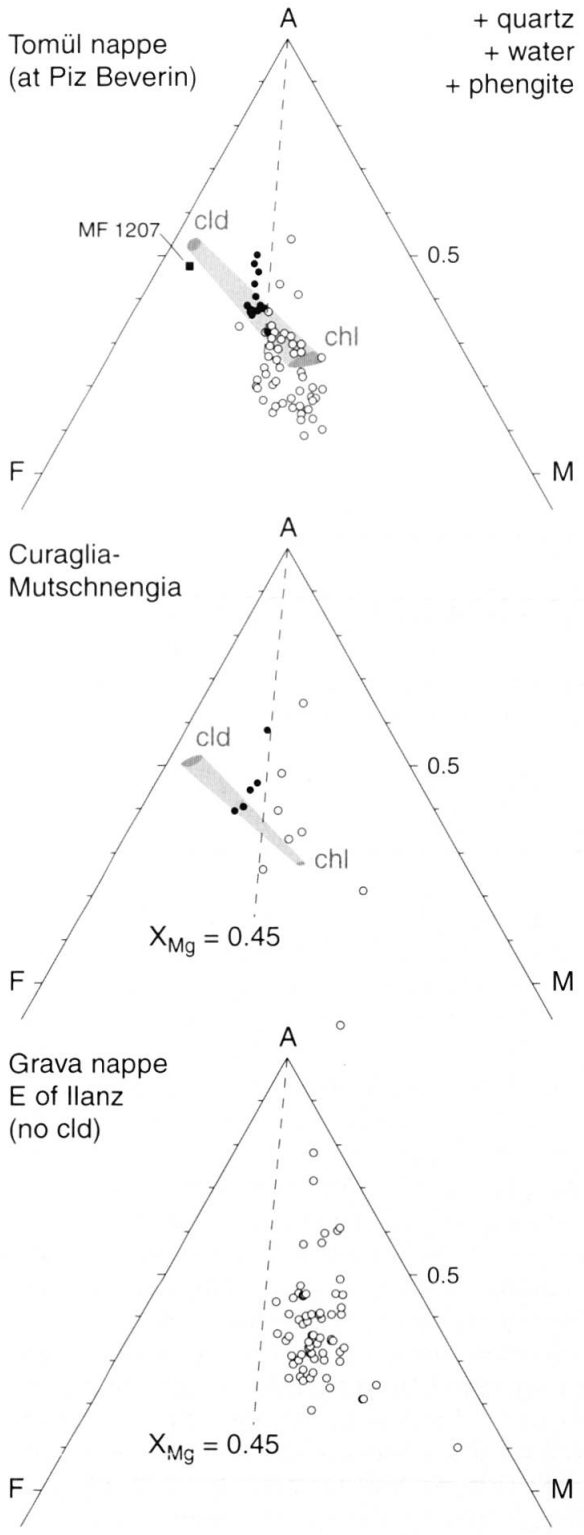

Fig. 6 Distribution of bulk rock composition for the Tomül nappe profile (top), for Curaglia/Mutschnengia (middle), and the Grava nappe profile (bottom) in an AFM diagram (with projection through phengite). Black dots indicate chloritoid-bearing samples, open circles are samples without chloritoid. The areas of chlorite (chl) and chloritoid (cld) composition are outlined by dark grey patches, while the areas of potential tie-lines between chlorite and chloritoid are indicated by light grey colour. The dashed line in all diagrams indicates a X_{Mg} of 0.45. In the Grava nappe, no chloritoid was detected.

er, is found between cld-chl pairs aligned in the main schistosity and those not aligned, in qtz-rich layers within the Bündnerschiefer. In contrast, the data set of cld-chl pairs at Curaglia exhibits a restricted variation in X_{Mg} for both phases (Fig. 7, bottom), indicating exchange equilibrium in the sample.

A source of uncertainty in the temperature estimates arises from the Mn contents of the measured chloritoids. VIDAL et al. (1999) restricted their data set to cld analyses with <1 wt% MnO. This condition is also applicable to the cld analyses of Kunkels Pass and Curaglia, while in the Tomül nappe MnO in cld is generally >1% (Fig. 3). The influence of Mn on the empirical temperature calculation is not known. Furthermore, VIDAL et al. (1999) reported a strong increase of uncertainty for the temperature determination beyond values of $X_{Mg} < 0.1$ at 300 °C and <0.2 at 700 °C. The X_{Mg} of a restricted number of chloritoids used for thermometry are around 0.1, which means that some temperature determinations may have large uncertainties. The differences in uncertainty were not considered when calculating the mean temperatures for the different localities.

Alternatively, chl composition alone can be used to roughly estimate the formation temperature on the basis of the empirical thermometer of CATHELINEAU (1988). Temperatures have to be considered with caution, because this thermometer was calibrated on chlorites from a hydrothermal field, and the observed process of Al incorporation with increasing temperature is suggested to represent a measure for reaction progress rather than equilibrium (ESSENE and PEACOR, 1995). Temperature calculations were restricted to chlorite with $(CaO+Na_2O+K_2O) < 0.2$ wt% to avoid non-chloritic interlayers (JIANG et al., 1994). For the Tomül nappe samples, a mean chl temperature of 380 ± 34 °C (2σ, n = 22) is derived, while chlorites from Curaglia give 387 ± 25 °C (n = 4). Chl temperatures are slightly lower than those derived from the chl-cld thermometry, but for both localities the results agree within 2σ. The combination of the temperature determinations give estimates of 400 ± 50 °C for the Tomül nappe profile, and 400 ± 40 °C for Curaglia.

Because the Helvetic shales from Kunkels Pass contain no chl, temperature estimates for these samples rely on the mineral assemblage, data on the maturation of organic matter by ERDELBROCK (1994), on illite crystallinity (WANG et al., 1996), and the state of reset of zircon FT ages (RAHN et al., 2000). These independently estimated maximum temperatures all lie in the range of 300–350 °C and thus are distinctly lower than calculated for the other two localities. We note that

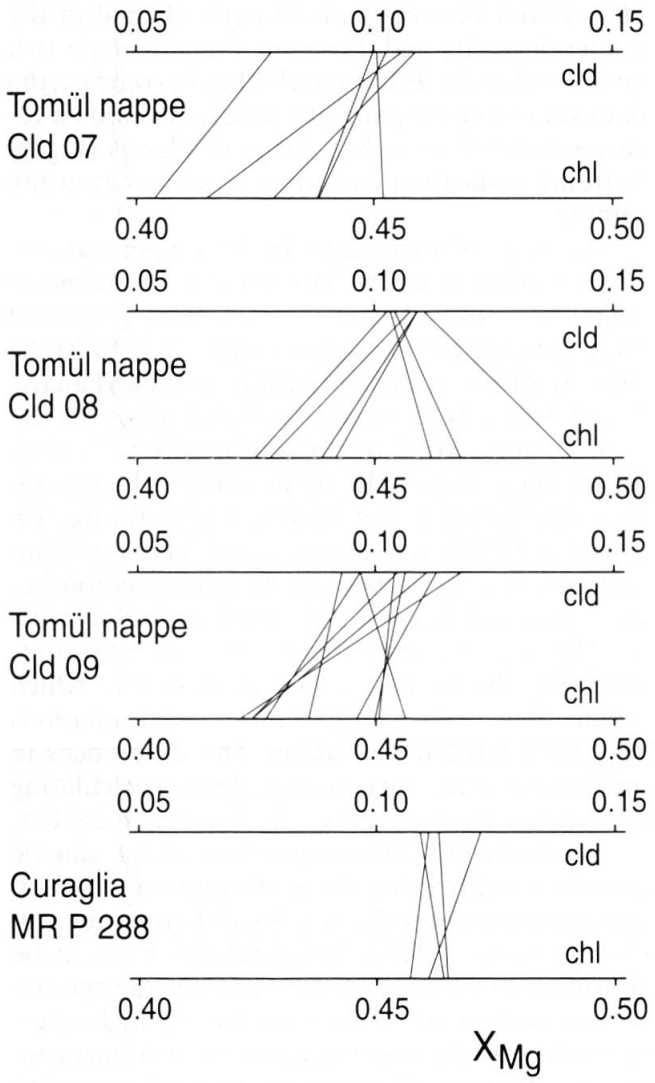

Fig. 7 Comparison of the X_{Mg} homogeneity of chlorite/chloritoid pairs used for temperature estimations sensu VIDAL et al. (1999).

cld from Kunkels Pass is only faintly lower in MgO content (1–1.8 wt%) than cld from the Tomül nappe and Curaglia (1.1–2.1 wt%) and cld from the Engadine window (1.6–1.9 wt%, BOUSQUET, 1998). For comparison, cld from the Lukmanier Pass area (uppermost greenschist to lower amphibolite facies), show MgO contents between 2.7 and 6.3 wt% (FREY, 1969).

GOFFÉ and OBERHÄNSLI (1992) and BOUSQUET et al. (1998) described the formation of cld in Bündnerschiefer as a result of a temperature increase and therefore prograde replacement of ferrocarpholite at pressures of 0.6–0.8 GPa (Val Lugnez) and 1.1–1.4 GPa (Engadine window). According to their calculations, the transition from ferrocarpholite to cld-bearing assemblages corresponds to temperatures of 300 °C (Val Lugnez) and 375 °C (Engadine window), which is consistent with peak temperatures presented here. Ferrocarpholite, however, has not been observed in any of our samples from the Tomül nappe profile, from Curaglia and Kunkels Pass, and there are no signs of cld growing as pseudomorphs after ferrocarpholite. Ferrocarpholite has been reported from neighbouring Val Lugnez (GOFFÉ and OBERHÄNSLI, 1992) and also from Safien valley, i.e. below the investigated Tomül nappe profile (BOUSQUET and OBERHÄNSLI, pers. comm., PETROVA et al., 2002).

5.3. BAROMETRY

In view of a potential high-pressure formation of cld from ferrocarpholite in the Bündnerschiefer, pressure is an important physical parameter to consider. In Bündnerschiefer phengite is aligned in the main schistosity, together with cld and chl, and these phases are considered to form a common assemblage. Phengitic mica in the Bündnerschiefer shows a variation in Si contents of 3.05–3.42. On the basis of the reaction

$$5 \text{ muscovite (ms)} + 6 \text{ albite} + \text{chl} + 2 \text{ qtz} + 2 \text{ H}_2\text{O} \rightarrow 5 \text{ celadonite (cel)} + 6 \text{ pg}$$

and the temperatures derived above, this should correspond to pressures between 0.3 and 0.9 GPa (OBERHÄNSLI et al., 1995; BOUSQUET et al., 1998). However, the analysed phengitic mica has compositional features that render this pressure determination doubtful (Fig. 5). First, the total content of interlayer cations (based on 22 oxygens) does not exceed 1.5, indicating a maximum occupancy of the interlayer of 75%. Such values are typical of very low-grade illite with smectite intergrowth (HUNZIKER et al., 1986). A positive charge balance within the tetrahedral and octahedral sheets compensates the interlayer charge deficiency, resulting in a neutral total charge balance.

Second, the pg content in the phengitic analyses may result from submicroscopic pg/phe intergrowth, and this has a strong influence on the Si content. The observed correlation between Na and Si (Fig. 5), and the fact that one pg analysis has a Si content of exactly 3.0, supports the idea of a potential influence of pg intergrowth. Although no Na-poor analyses were obtained, this observed trend may be used to estimate the Si content of pg-free phengite. Assuming that pg interlayers is the only cause for Si variation, the Si content of Na-free phengite is slightly above 3.4 (Fig. 5), indicating pressures of 0.7–0.9 GPa, in line with elevated pressure for mica formation. However, this estimated phengite composition yields a large interlayer deficiency, typical of sub-greenschist facies white mica.

Third, the correlation between Si content and (Fe+Mn+Mg) in phengite from Bündnerschiefer does not indicate a cel exchange. Instead the amount of incorporated bivalent cations follows an exchange vector that indicates substitution of two bivalent cations for one Si (plus a vacancy). Other valences such as Fe^{3+} or Mn^{3+} are unlikely because of the charge balance, as is the idea of a combined intergrowth of phengite, chlorite and quartz, in view of the observed clear trend. For the present assemblages, we therefore doubt that reliable estimates of temperature (BLENCOE et al., 1992) and pressure (OBERHÄNSLI et al., 1995) can be obtained from the mica analyses. Hence it is not possible to prove or disprove the high pressure origin of the present assemblage with these methods.

5.4. FORMATION OF CLD

Based on the comparison between bulk rock and mineral compositions, the formation of cld seems to be influenced by mainly three compositional components: (1) Rocks have to be rich in Al. Cld-bearing samples commonly plot above a tie-line between chl and cld in AFM diagrams. An exception to this rule may apply to samples without chl (MF 1207, Fig. 6). (2) Cld-bearing samples are poor in carbonate phases, suggesting that the cld-forming reaction depends on the composition of the involved fluid. It may be assumed that the kinetics of fluid saturation with CO_2 at the estimated temperatures were slow and that the amount of released CO_2 was therefore not only dependent on the presence of a carbonate phase, but also on its relative amount and the volume of fluid flow at that time. (3) The formation of cld is distinctly sensitive to bulk rock X_{Mg} values. For all three localities with extended bulk rock data, a critical X_{Mg} value of 0.45 is observed (Fig. 6) that separates cld-bearing samples (X_{Mg}<0.45) from cld-free ones. This critical value seems to be independent of the (relatively low) Mn contents of the bulk rock and chloritoid. The linear relationship between bulk rock and cld Mn content suggests that cld contains most of the Mn in the Bündnerschiefer.

When comparing cld-bearing and cld-free samples, no obvious dependence on the proportions of (clay fraction) sheet silicates is seen (Fig. 2). This suggests that none of the sheet silicate phases, in particular chl, is involved in cld formation. Prl as one of the possible precursors in cld formation (e.g. FREY and WIELAND, 1975) is absent and has not been found in Bündnerschiefer of lower grade further east (THUM and NABHOLZ, 1972; FERREIRO MÄHLMANN, 1994). Hematite, which was proposed by FREY (1969) as an important source of Fe, is absent in the cld-bearing Quartenschiefer, and neither the green nor violet samples typical of the same stratigraphic unit contain cld. Hematite is, however, an important accessory mineral in cld-bearing Bündnerschiefer. FREY (1969) suggested that a TiO_2 phase should form when hematite breaks down to form cld. Small amounts of a TiO_2 phase (polymorph not specified) are commonly present in all of our cld-bearing samples from the Tomül nappe. Magnetite, however, which was proposed by BUCHER and FREY (1994) as a potential product of cld formation, has not been found in any sample.

From the bulk rock data (Table 3), it is evident that the only elements of importance are Al, (Fe+Mn+Mg), K and Na. Qtz and H_2O can be assumed as being present in excess, while Ca-phases are present in cld-bearing samples in minor amounts only. K and Na in cld-bearing samples are mostly restricted to white mica phases and feldspars, and the formation and replacement of Na- and K-micas should always be linked to the consumption or formation of the corresponding feldspar phases, which are commonly present in minor amounts. Thus, the assemblage may be reduced to a quaternary system containing the phases ab, cld, chl, kfs, ms, pg, and a Fe-phase, which for Bündnerschiefer is hematite, and for Quartenschiefer may have been hematite or a phase with divalent Fe, such as pyrite (weathered). In addition to these phases, prl was added, because (i) it is a common phase in low-grade metapelites (e.g. PHILLIPS, 1988; GHENT et al., 1989), (ii) it has been proposed as a precursor of cld (e.g. FREY and WIELAND, 1975), and (iii) it allows to evaluate the importance of the Al contents in the rocks for the formation of cld.

The resulting quaternary system (p = 8, c = 4, f = –2) may be simplified graphically by projection along the tetrahedron edge between kfs and ab to result in a modified AKF system with K' = ($KAlO_2$+$NaAlO_2$) and F' = (FeO+MgO+MnO) (Fig. 8). Seven reactions involving cld may be formulated in this system:

chl = cld + Fe phase + qtz + H_2O (1)

Fe-phase + prl = cld + qtz (2)

(as proposed in a similar form by PHILLIPS, 1988)

chl + prl = cld + qtz + H_2O (3)

(as mapped by FREY and WIELAND, 1975)

Fe phase + ms/pg + qtz = cld + kfs/ab + H_2O (2 reactions) (4), (5)

chl + ms/pg + qtz = cld + kfs/ab + H_2O (2 reactions) (6), (7)

Table 3 Bulk rock chemical analyses of major elements from all cld-bearing samples from Tomül nappe, Curaglia and Kunkels Pass. n. m. = not measured.

Sample	MB 11.1	MB 11.2	MB 13	MB 20.1	MB 22.1	MB 22.2	MB 24.1	MB 25.1	CC 12.1	Cld 02
locality	Tomül nappe	Tomül nappe	Tomül nappe	Tomül nappe	Tomül nappe	Tomül nappe	Tomül nappe	Tomül nappe	Tomül nappe	Tomül nappe
SiO_2	65.48	49.08	67.90	63.01	60.43	52.96	58.99	60.31	72.23	65.66
TiO_2	0.64	1.18	0.71	0.75	0.80	1.01	0.78	0.53	0.58	0.73
Al_2O_3	18.68	28.23	17.63	19.35	20.39	23.21	20.55	14.73	14.23	17.71
Fe_2O_3	3.85	6.29	5.12	5.14	6.77	8.97	7.07	5.41	3.90	5.49
MnO	0.05	0.15	0.14	0.12	0.26	0.24	0.21	0.14	0.08	0.19
MgO	1.19	1.82	1.58	1.72	1.85	2.65	2.03	2.05	1.41	1.77
CaO	0.53	0.27	0.16	0.23	0.10	0.15	0.24	5.03	0.23	0.20
Na_2O	0.53	1.61	0.82	0.79	0.69	0.87	0.86	0.56	0.87	1.34
K_2O	3.16	3.92	2.63	3.25	2.97	2.99	3.01	2.13	2.33	3.71
P_2O_5	0.14	0.19	0.13	0.09	0.10	0.12	0.16	0.05	0.12	0.08
LOI	3.44	5.33	3.09	3.82	3.92	4.90	4.12	7.12	2.80	4.32
Σ	97.69	98.07	99.91	98.27	98.28	98.07	98.02	98.06	98.78	101.20

Sample	Cld 07	Cld 08	Cld 09	MR P 288	MR P 305d	MR P 305e	MR P 305f	MR P 308	MF 1207
Locality	Tomül nappe	Tomül nappe	Tomül nappe	Curaglia	Mutsch-nengia	Mutsch-nengia	Mutsch-nengia	Mutsch-nengia	Kunkels Pass
SiO_2	69.09	61.99	56.19	61.82	59.74	64.48	53.35	67.94	66.97
TiO_2	0.63	0.80	0.91	1.06	1.00	1.15	1.05	0.97	0.90
Al_2O_3	16.15	21.39	23.82	21.66	20.56	20.07	23.09	15.30	17.50
Fe_2O_3	5.23	4.58	6.05	5.83	6.89	4.67	10.44	6.65	5.49
MnO	0.19	0.14	0.12	0.01	0.04	0.03	0.05	0.01	0.05
MgO	1.56	1.27	1.77	1.98	2.00	1.48	2.80	1.60	0.38
CaO	0.18	0.16	0.20	0.19	1.07	0.19	0.51	0.22	0.27
Na_2O	0.79	1.23	1.34	2.21	0.52	0.52	0.35	0.60	0.35
K_2O	2.45	3.41	3.71	1.35	2.92	3.63	2.85	2.18	3.18
P_2O_5	0.06	0.08	0.10	0.03	0.28	0.09	0.28	0.11	0.07
LOI	3.57	4.82	5.65	3.85	n.m.	n.m.	n.m.	n.m.	4.74
Σ	99.90	99.87	99.86	99.99	95.02	96.31	94.77	95.58	99.90

Consideration of the celadonite component in muscovite (phe), leads to further reactions:

$$\text{chl} + \text{ms} = \text{cld} + \text{celadonite} + \text{qtz} + H_2O \quad (8)$$
$$\text{phe} + \text{qtz} = \text{cld} + \text{kfs} + \text{prl} + H_2O \quad (9)$$

For Bündnerschiefer of the Tomül nappe, the cld precursors may have been dioctahedral chlorite (sudoite, su) or ferrocarpholite (Fe car), which leads to the reactions

$$\text{su} = \text{cld} + \text{qtz} + H_2O \quad (10)$$
$$\text{Fe car} = \text{cld} + \text{qtz} + H_2O \quad (11)$$

With one exception (reaction 2), all above reactions represent dehydration processes, occurring during prograde evolution. Their prograde character and the fact that cld represents the mineral of the highest metamorphic grade in the investigated parageneses strongly suggest that cld was formed under maximum T conditions or equilibrated with rising temperatures (missing zonation). Reactions 4–7 all suggest the formation of feldspars next to cld. On the basis of optical investigations and back-scattered imaging, these reactions seem to be improbable, because grains of feldspar were only occasionally detected in all samples, but never in close vicinity of cld. The observed dependence of cld formation on the bulk rock X_{Mg} further suggests that Fe and Mg for the formation of cld has to come from a phase that is able to incorporate and supply both elements. In that sense, reactions 1, 2, 4, and 5 are unlikely, because none of the known Fe phases include major amounts of Mg.

From graphical evaluations (Fig. 8), it can be deduced that the tie-line between chl and phe (ms) played an important limit to the occurrence of cld: At Curaglia/Mutschnengia, the tie-line sharply separates cld-bearing from cld-free samples. (Note that white mica was assumed to be ms endmember because compositional data are not reliable, as shown above.) In Bündnerschiefer, phe analyses are strongly shifted downwards due

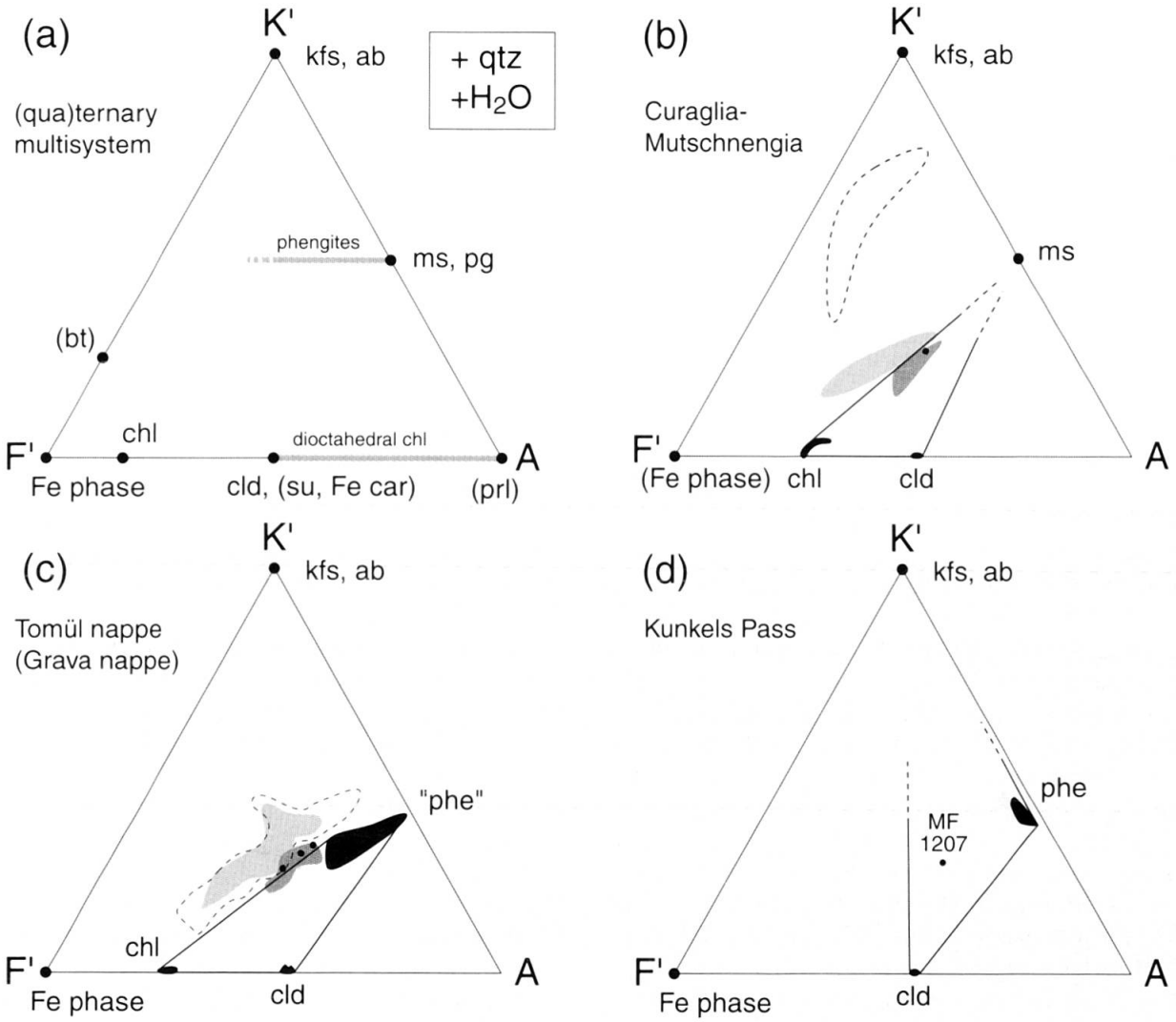

Fig. 8 Modified AKF diagrams for the investigated localities. (a) Geometry of a quaternary multisystem with projection along the upper $KAlO_2$–$NaAlO_2$ edge with K' = $KAlO_2$ + $NaAlO_2$, F' = FeO + MgO + MnO, and the phases albite (ab), biotite (bt), chlorite (chl), chloritoid (cld), ferrocarpholite (Fe car), a Fe-bearing phase (not specified), K-feldspar (kfs), muscovite (ms), paragonite (pg), pyrophyllite (prl), and sudoite (su). Phases in brackets were not observed, but are given for completion. (c) bulk rock and mineral data from the Bündnerschiefer. Irregular black areas: ranges of mineral composition (labelled), dark grey: cld-bearing samples from the Tomül nappe, light grey: Tomül nappe samples without cld, small black dots: cld-bearing samples investigated for mineral composition, dashed outline: compositional range of Grava nappe samples. (b) mineral and bulk rock data from Curaglia/Mutschnengia. Irregular black areas: ranges of mineral composition (labelled, no white mica analysis available), dark grey: cld-bearing Quartenschiefer, light grey: cld-free Quartenschiefer, small black dot: composition of investigated sample (MR P 288), dashed outline: Liassic shales with no cld. (d) mineral and bulk rock data from Kunkels Pass. Black areas: ranges of mineral composition (labelled), small black dot: composition of investigated sample (MF 1207). For the Bündnerschiefer and Curaglia/Mutschnengia, a paragenesis cld-chl-phe is indicated, while for Kunkels Pass, a paragenesis cld-phe-kfs is indicated. For discussion see text.

to interlayer deficiency. As a consequence, the bulk rock analyses of the three investigated samples plot outside the observed assemblage chl-phe-cld. However, all cld-free samples plot above the phe-chl tie-line, as do all samples from the Grava nappe (no cld). The obvious dependence on chl and white mica composition suggests that in samples from these localities, these two phases played an important role in cld formation (reaction 8). Because white mica analyses indicate intergrowths of at least two phases (ms and pg), and white micas were not measured in samples without chloritoid, the relevance of reaction 8 cannot be further evaluated.

Fe car is known from Bündnerschiefer at surrounding localities (OBERHÄNSLI et al., 1995; BOUSQUET et al., 1998), making reaction 11 an interesting alternative to reaction 8. Sudoite has not yet been reported from the Bündnerschiefer shales, and prl is nearly totally absent in Bündner-

schiefer of lower grade (THUM and NABHOLZ, 1972; FERREIRO MÄHLMANN, 1994, 1996). If prl was not involved in cld formation, reaction 8 represents the only alternative to form cld from a non-HP precursor.

In the Infrapenninic Gotthard nappe cover, no HP relics are known up to now. Due to the absence of newly formed feldspar, prl and large quantities of a Fe phase, as well as the strong dependence of cld presence on the chl-ms tie-line, reactions 3 and 8 are suggested to be most relevant. The absence of pyrophyllite would suggest that reaction 3 was completed by the total consumption of this phase, while 8, a continuous reaction, is expected to produce zoned mineral grains, if it was operative over an extended period. We have no reason to favor one of these reactions over the other.

For the Helvetic sample from Kunkels Pass, a reaction consuming chl is suggested (reactions 1, 3, 6, 7, and 8). With the exception of minor pyrite, no Fe bearing phase is present in samples without cld from the same locality, which would support reaction 1 to have played an important role at this locality. Newly formed feldspar has not been detected, but because the composition of the investigated sample plots outside the triangle cld-ms-prl, the stable assemblage is assumed to be cld-ms-kfs (pg is absent, Fig. 8). The presence of prl in similar rocks of lower grade in the Helvetics strongly supports the former suggestion of FREY and WIELAND (1975) that cld was formed at the expense of prl and chl. However, reaction 8 may be an alternative to be tested with better white mica analyses from cld-bearing and -free samples.

6. Conclusions

The comparison of three occurrences of cld within different units of low greenschist facies grade from the eastern Central Alps reveals a very narrow chemical variability for this mineral close to its Fe end-member, and a restricted compositional range for associated chl. Occurrences of cld at Kunkels Pass (Helvetic belt) and Curaglia (Gotthard nappe sediment cover) are the result of a syn- to post-deformational metamorphic overprint in Early Oligocene time reaching 300–350 °C at Kunkels Pass and 400±40 °C at Curaglia. At the Tomül nappe profile (North Penninic Bündnerschiefer), cld grew pre-D2 at 400±50 °C, but formed earlier than in the neighbouring Infrapenninic and Helvetic units.

In the Bündnerschiefer samples investigated, no Fe car (or pseudomorphs) have been found together with cld, which would have supported cld growth at the expense of car at elevated pressures (GOFFÉ and OBERHÄNSLI,1992; OBERHÄNSLI et al., 1995; BOUSQUET et al., 1998), but such a reaction would fit in the pattern of regional and local observations. A formation of cld by breakdown of prl (FREY and WIELAND, 1975), established from regional mapping within the Helvetic belt, is not likely, because prl as a potential precursor of cld is absent in lower-grade Bündnerschiefer further to the east. An alternative reaction is proposed, with formation of cld and a more celadonitic white mica at the expense of chl and muscovitic white mica. For Quartenschiefer from the Gotthard nappe sedimentary cover and for Jurassic shales from Kunkels Pass, the same reaction is an alternative to cld formation at the expense of prl and chl (FREY and WIELAND, 1975). In the case of the latter reaction, the amount of chl (Kunkels Pass) or prl (Curaglia) would have been the limiting factor for cld production.

The Fe/Mg ratio of the bulk rock represents an important condition in the formation of cld, and this ratio is related to the composition of chl and phe (Fig. 8). The role of Mn in cld formation is not known, and Mn in cld is controlled by the bulk rock Mn contents. For cld in Bündnerschiefer, Mn contents are in the range of Mg contents. Since the influence of Mn on chl-cld thermometry (VIDAL et al., 1999) is unknown, the derived chl-cld temperatures for the Tomül nappe profile are considered preliminary.

Caution has to be applied also when using phengite analyses to estimate pressure in low-grade Bündnerschiefer. White micas from the North Penninic Tomül nappe profile show compositional variations incompatible with a cel exchange. The presence of pg/phe intergrowth is inferred for all analyses, leading to depleted Si contents and incorrect pressure determinations.

Acknowledgements

This paper is dedicated to our co-author, Martin Frey, who sowed the seed of this project, but is no longer among us to see the harvest. We owe our thanks to Hiltrud Müller for her immense advice and help with the electron microprobe, and to Isolde Schmidt for the XRD and XRF analyses at Freiburg University. Our work has profited from discussions with R. Bousquet and J. Mullis. Reviews by M. Engi, R. Ferreiro Mählmann, R. Oberhänsli, S.Th. Schmidt, and T. Theye helped to substantially improve the content of the manuscript. M. Rahn was financially supported by grant Ra 704/3-1 of the Deutsche Forschungsgemeinschaft, M. Steinmann acknowledges financial support by the Swiss Nationalfonds grants no. 21-25272.88 and 2-77-125-91.

References

BEARTH, P. (1967): Die Ophiolithe der Zone Zermatt-Saas Fee. Beitr. Geol. Karte Schweiz 132, 130 pp.

BECKER, H. (1992): Garnet peridotite and eclogite Sm–Nd mineral ages from the Lepontine dome (Ticino, Switzerland): New evidence for an Eocene high pressure metamorphism in the Central Alps. Beih. Eur. J. Mineral. 4, p. 22.

BLENCOE, J.G., GUIDOTTI, C.V. and SASSI, F.P. (1992): An improved set of solvus data for synthetic, binary paragonite-muscovite micas. Eos Transactions 73, p. 327.

BOUSQUET, R. (1998): L'exhumation des roches métamorphiques de haute pression – basse température: de l'étude de terrain à la modélisation numérique. Unpubl. Ph.D. thesis, Université de Paris Sud, 279 pp.

BOUSQUET, R., OBERHÄNSLI, R., GOFFÉ, B., JOLIVET, L. and VIDAL, O. (1998): High-pressure-low-temperature metamorphism and deformation in the Bündnerschiefer of the Engadine window: implications for the regional evolution of the eastern Central Alps. J. Metamorphic Geol. 16, 657–674.

BUCHER, K. and FREY, M. (1994): Petrogenesis of Metamorphic Rocks. Springer, Berlin, 318 pp.

CATHELINEAU, M. (1988): Cation site occupancy in chlorites and illites as a function of temperature. Clay Min. 23, 471–485.

ERDELBROCK, K. (1994): Diagenese und schwache Metamorphose im Helvetikum der Ostschweiz (Inkohlung und Illit-"Kristallinität"). Unpubl. Ph.D. thesis, TH Aachen, 220 pp.

ESSENE, E.J. and PEACOR, D.R. (1995): Clay mineral thermometry – A critical perspective. Clay Clay Min. 43, 540–553.

ETTER, U. (1987): Stratigraphische und strukturgeologische Untersuchungen im gotthardmassivischen Mesozoikum zwischen dem Lukmanierpass und der Gegend von Ilanz. Unpubl. Ph.D. thesis Universität Bern, 162 pp.

FERREIRO MÄHLMANN, R. (1994): Zur Bestimmung von Diagenesehöhe und beginnender Metamorphose – Temperaturgeschichte und Tektogenese des Austroalpins und Südpenninikums in Vorarlberg und Mittelbünden. Frankfurter geowissenschaftliche Arbeiten, Serie C, 14, 498 pp.

FERREIRO MÄHLMANN, R. (1996): Das Diagenese-Metamorphose-Muster von Vitrinitreflexion und Illit-"Kristallinität" in Mittelbünden und im Oberhalbstein; Teil 2, Korrelation kohlenpetrographischer und mineralogischer Parameter. Schweiz. Mineral. Petrogr. Mitt. 76, 23–46.

FREY, M. (1969): Die Metamorphose des Keupers vom Tafeljura bis zum Lukmanier-Gebiet. Beitr. Geol. Karte Schweiz 129, 78 pp.

FREY, M. (1969): A mixed layer paragonite/phengite of low-grade metamorphic origin. Contrib. Mineral. Petrol. 24, 63–65.

FREY, M. and WIELAND, B. (1975): Chloritoid in autochthon-parautochthonen Sedimenten des Aarmassivs. Schweiz. Mineral. Petrogr. Mitt. 55, 407–418.

FREY, M., DESMONS, J. and NEUBAUER, F. (1999): The new metamorphic map of the Alps: Introduction. Schweiz. Mineral. Petrogr. Mitt. 79, 1–4.

FREY, M. and FERREIRO MÄHLMANN, R. (1999): Alpine metamorphism of the Central Alps. Schweiz. Mineral. Petrogr. Mitt. 79, 135–154.

GEBAUER, D., GRÜNENFELDER, M., TILTON, G., TROMMSDORFF, V. and SCHMID, S. (1992): The geodynamic evolution of garnet peridotites, garnet pyroxenites and eclogites of Alpe Arami and Cima di Gagnone (Central Alps): from Early Proterozoic to Oligocene. Schweiz. Mineral. Petrogr. Mitt. 72, 107–112.

GHENT, E.D., STOUT, M.Z. and FERRI, F. (1989): Chloritoid-paragonite-pyrophyllite and stilpnomelane-bearing rocks near Blackwater Mountain, Western Rocky Mountains, British Columbia. Can. Mineral. 27, 59–66.

GOFFÉ, B. and OBERHÄNSLI, R. (1992): Ferro- and magnesiocarpholite in the "Bündnerschiefer" of the eastern Central Alps (Grisons and Engadine window). Eur. J. Mineral. 4, 835–838.

GOFFÉ, B. and BOUSQUET, R. (1997): Ferrocarpholite, chloritoide et lawsonite dans les métapelites des unités du Versoyen et du Petit St. Bernard (zone valaisanne, Alpes occidentales). Schweiz. Mineral. Petrogr. Mitt. 77, 137–147.

HUNZIKER, J.C., FREY, M., CLAUER, N., DALLMEYER, R.D., FRIEDRICHSEN, H., FLEHMIG, W., HOCHSTRASSER, K., ROGGWILER, P. and SCHWANDER, H. (1986): The evolution of illite to muscovite: mineralogical and isotopic data from the Glarus Alps, Switzerland. Contrib. Mineral. Petrol. 92, 157–180.

JIANG, W.T., PEACOR, D.R. and BUSECK, P.R. (1994): Chlorite geothermometry? Contamination and apparent octahedral vacancies. Clay Clay Min. 42, 593–605.

LEHNER, P., MÜLLER, S. and TRÜMPY, R. (1997): Deep structure of the Swiss Alps; an introduction. In: PFIFFNER, O.A., LEHNER, P., HEITZMANN, P., MÜLLER, S. and STECK, A. (eds): Results of NRP 20; deep structure of the Swiss Alps. Birkhäuser, Basel, 1–9.

MAYERAT, A.-M. (1986): Aspects de la déformation des massifs du Tavetsch et du Gotthard au Val Medel. Eclogae geol. Helv. 79, 246–251.

MILNES, A.G. and PFIFFNER, O.A. (1977): Structural development of the Infrahelvetic Complex, eastern Switzerland. Eclogae geol. Helv. 70, 83–95.

NIGGLI, E. and NIGGLI, C. (1965): Karten der Verbreitung einiger Mineralien der alpidischen Metamorphose in den Schweizer Alpen (Stilpnomelan, Alkali-Amphibol, Chloritoid, Staurolith, Disthen, Sillimanit). Eclogae geol. Helv. 58, 335–368.

OBERHÄNSLI, R. (1994): Subducted and obducted ophiolites of the Central Alps: Palaeotectonic implications deduced by their distribution and metamorphic overprint. Lithos 33, 109–118.

OBERHÄNSLI, R., GOFFÉ, B. and BOUSQUET, R. (1995): Record of a HP-LT metamorphic evolution in the Valais zone: Geodynamic implications. In: LOMBARDO, B. (ed.): Studies on metamorphic rocks and minerals of the Western Alps. A Volume in Memory of Ugo Pognante. Boll. Museo Regionale Szienze Naturali. Torino, 13, 221–239.

PETROVA, T.V., FERREIRO MÄHLMANN, R., STERN, W.B. and FREY, M. (2002): Application of combustion and DTA-TGA analysis to the study of metamorphic organic matter. Schweiz. Mineral. Petrogr. Mitt. 82, 33–53.

PFIFFNER, O.A. (1978): Der Falten- und Kleindeckenbau im Infrahelvetikum der Ostschweiz. Eclogae geol. Helv. 71, 61–84.

PFIFFNER, O.A. (1986): Evolution of the north Alpine foreland basin in the Central Alps. Spec. Publ. Int. Ass. Sediment. 8, 219–228.

PHILLIPS, G.N. (1988): Widespread fluid infiltration during metamorphism of the Witwatersrand goldfields: generation of chloritoid and pyrophyllite. J. Metamorphic Geol. 6, 311–332.

PROBST, P. (1980): Die Bündnerschiefer des nördlichen Penninikums zwischen Valser Tal und Passo di San Giacomo. Beitr. geol. Karte Schweiz N.F. 153, 63 pp.

RAHN, M.K., MULLIS, J., ERDELBROCK, K and FREY, M. (1995): Alpine metamorphism in the North Helvetic flysch of the Glarus Alps, Switzerland. Eclogae geol. Helv. 88, 157–178.

RAHN, M.K., MULLIS, J. and HURFORD, A.J. (2000): No Alpine zircon FT ages in the Helvetics? 75th Ann. Meet. Swiss Soc. Mineral. Petrol., Winterthur, Abstract volume.

RING, U. (1992): The Alpine geodynamic evolution of Penninic nappes in the eastern Central Alps: geothermobarometric and kinematic data. J. Metamorphic Geol. 10, 33–53.

SCHMID , S.M., RÜCK, P. and SCHREURS, G. (1990): The significance of the Schams nappes for the reconstruction of the palaeotectonic and orogenic evolution of the Penninic zone along the NFP-20 East traverse (Grisons, eastern Switzerland). In: ROURE, F., HEITZMANN, P. and POLINO, R. (eds): Deep structure of the Alps. Mém. Soc. Géol Fr. 156, 263–287.

SCHMID, S.M., PFIFFNER, O.A. and SCHREURS, G. (1997): Rifting and collision in the Penninic zone of eastern Switzerland. In: PFIFFNER, O.A., LEHNER, P., HEITZMANN, P., MÜLLER, S. and STECK, A. (eds): Results of NRP 20; deep structure of the Swiss Alps. Birkhäuser, Basel, 160–185.

SCHREURS, G. (1991): Structural analysis of the Schams nappes and adjacent tectonic units in the Penninic zone (Grisons, SE-Switzerland). Mitt. geol. Inst. ETH u. Univ. Zürich N.F. 283, 204 pp.

SCHREURS, G. (1993): Structural analysis of the Schams nappes and adjacent tectonic units: implications for the orogenic evolution of the Penninic zone in eastern Switzerland. Bull. Soc. géol. France 164, 415–435.

STAMPFLI, G.M. and MARCHANT, R.H. (1997): Geodynamic evolution of the Tethyan margins of the Western Alps. In: PFIFFNER, O.A., LEHNER, P., HEITZMANN, P., MÜLLER, S. and STECK, A. (eds): Results of NRP 20; deep structure of the Swiss Alps. Birkhäuser, Basel, 223–239.

STAMPFLI, G.M., MOSAR, J., MARQUER, D., MARCHANT, R., BAUDIN, T. and BOREL, G. (1998): Subduction and obduction processes in the Swiss Alps. Tectonophysics 296, 159–204.

STEINMANN, M.C. (1994a): Die nordpenninischen Bündnerschiefer der Zentralalpen Graubündens: Tektonik, Stratigraphie und Beckenentwicklung. Unpubl. Ph.D. thesis, ETH Zürich, nr. 10668, 220 pp.

STEINMANN, M. (1994b): Ein Beckenmodell für das Nordpenninikum der Ostschweiz. Jb. Geol. B.-A. Wien 137, 675–721.

STEINMANN, M. and STILLE, P. (1999): Geochemical evidence for the nature of the crust beneath the eastern North Penninic basin of the Mesozoic Tethys ocean. Geol. Rundsch. 87, 633–643.

THUM, I. and NABHOLZ, W. (1972): Zur Sedimentologie und Metamorphose der penninischen Flysch- und Schieferabfolgen im Gebiet Prättigau-Lenzerheide-Oberhalbstein. Beitr. Geol. Karte Schweiz 144, 55 pp.

TROMMSDORFF, V., PICCARDO, G.B. and MONTRASIO, A. (1993): From magmatism through metamorphism to sea floor emplacement of subcontinental Adria lithosphere during pre-Alpine rifting (Malenco, Italy). Schweiz. Mineral. Petrogr. Mitt. 73, 191–203.

TRÜMPY, R. (1980): Geology of Switzerland – a guide book. Wepf, Basel, 104 pp.

TRÜMPY, R. (1988): A possible Jurassic–Cretaceous transform system in the Alps and the Carpathians. Geol. Soc. Am. Spec. Pap. 218, 93–109.

VIDAL, O., GOFFÉ, B., BOUSQUET, R. and PARRA, T. (1999): Calibration and testing of an empirical chloritoid-chlorite Mg-Fe exchange thermometer and thermodynamic data for daphnite. J. Metamorphic Geol., 17, 25–39.

WANG, H., FREY, M. and STERN, W.B. (1996): Diagenesis and metamorphism of clay minerals in the Helvetic Alps of Eastern Switzerland. Clay Clay Min. 44, 96–112.

WEH, M. (1998): Tektonische Entwicklung der penninischen Sediment-Decken in Graubünden (Prättigau bis Oberhalbstein). Unpubl. Ph.D. thesis, Basel University, 296 pp.

WEH, M. and FROITZHEIM, N. (2001): Penninic cover nappes in the Prättigau half-window (Eastern Switzerland): Structure and tectonic evolution. Eclogae geol. Helv. 94, 237–252.

ZIEGLER, W.H. (1956): Geologische Studien in den Flyschgebieten des Oberhalbsteins (Graubünden). Eclogae geol. Helv. 49, 1–78.

Manuscript received November 11, 2001; revision accepted July 22, 2002.
Editorial handling: M. Engi